

# Open Loop Control of a Hysteretic System with an Inverse Volterra with a DC Component

Vladimir Cortés Lerín<sup>1</sup>, Juan Alejandro Vazquez Feijoo<sup>2</sup>, Rodrigo Arturo Marquet Rivera<sup>2</sup>,  
Guillermo Urriolagitia Sosa<sup>2</sup>, Beatriz Romero Angeles<sup>2</sup>,  
Guillermo Urriolagoitia Calderón

<sup>1</sup> Instituto Politécnico Nacional,  
Centro Interdisciplinario de Investigación para el Desarrollo Integral Regional,  
Academia de Ingeniería,  
Mexico

<sup>2</sup> Instituto Politécnico Nacional,  
Escuela Superior de Ingeniería Mecánica y Eléctrica,  
Sección de estudios de Posgrado e Investigación,  
Mexico

javazquezfeijoo@yahoo.com.mx,  
{vcortezl, rmarquetr, gurriolagoitias, bromeroa, gurriolagoitiac}@ipn.mx

**Abstract.** This work proposes an open loop control for sensor systems with hysteresis. This control is achieved by the use of an equalization strategy consisting in connecting in tandem the system with its inverse Volterra. For real cases hysteresis is associated with the interchange of mechanic-electric energy in the sensing process. Though these systems are amplitude dependent, they still can be treated as Wiener kind systems and therefore a Postinverse Volterra can be built. A simulated accelerometer shows how to implement this control.

**Keywords.** Nonlinear systems, hysteresis, associated linear equations, Volterra transform.

## 1 Introduction

Sensors possess their very own dynamics that limits its accuracy and precision. A sensor close loop control is not applicable. Therefore, only open loop control can be intend to eliminate the signal modification associated to sensor dynamics. The sensor system is quite often nonlinear, involving indirect measuring such as the mean square root that for example gives the driving input for ultrasonic motors [1].

Much of the sensor systems involves interchange between electric-mechanic energy, e.g., by the use of piezoelectrostrictive elements that involves hysteresis. This piezoelectric hysteresis has been intended to be controlled by PID strategies as in [2] or fuzzy logic like in [3] or [4] that may be used for actuator systems but not for sensors. Other application involves the control of induction motors [7]. Most of the work on hysteresis has as objective the identification rather than the control e.g., [6, 7, 8].

The work reported here, implements a open loop control using an equalization strategy reported in [9]. The equalization process consists in connect in tandem the system with its inverse Volterra. The operators of the inverse Volterra are obtained from discrete model series so-called Associated Linear Equations (ALEs) [10]. A system with hysteresis is amplitude dependent, therefore it cannot be strictly considered a Volterra kind.

However, if the system contains underling linear system, it might be treated as a Volterra system which its nonlinear terms have amplitude dependent coefficients. Consider as a base of the model the general behavior of an accelerometer,

the source of nonlinearity (hysteresis) may be the piezoelectric element that provides information about deformation as Voltage.

The accelerometer then can be modeled as a linear system (structure) connected in tandem with a hysteretic element. The most suitable Volterra model is the Wiener kind [10]. In order to obtain a more realistic model, of an accelerometer, the model used in here, includes a resilient damping, treated by Associated Linear Equation [11, 15] just as it has been done in [12].

## 2 Identification of the Hysteretic Cycle

There are several methods to reveal the linear part of a hysteretic system, e.g., [7]. Though any of them may be used to identify the linear part of the system, because in this work, the system is available at any level, the structural damped system (linear in frequency) is simply extracted from low levels of excitation.

The identification is going to be discrete versions of the Associated Linear Equations (ALEs) known as the AutoRegressive with eXogenous inputs models (ARX) as reported in [13]. The general structure of a one degrees-of-freedom ARX model of a system with structural damping is:

$$y(i) = C_1y(i-1) + C_2y(i-2) + C_3x(i-1) + C_4s(i-1), \quad (1)$$

where  $s(i)$  is the auxiliary variable that accounts for the complex rigidity that is defined as:

$$s(t) = i \operatorname{sign}(\omega)y(t), \quad (2)$$

which is obtained in the frequency domain as it is done in [10]. For the Wiener system presented in here, the structural damped system does not change at any level of hysteresis. The saturation point is supposed to be well into the elastic range of the structure.

At a given level, in which the hysteresis produces nonlinear behavior, the nonlinear system is modeled as two polynomials of third degree. Each one modeling the system when the output signal has a positive or negative slope. Then:

$$u(i) = Pu_1y^3(i) + Pu_2y^2(i) + Pu_3y(i) + Pu_4, \quad (3a)$$

$$v(i) = Pv_1y^3(i) + Pv_2y^2(i) + Pv_3y(i) + Pv_4. \quad (3b)$$

Both  $Pv$  and  $Pu$  are vectors of coefficients that change as the input level changes.

## 3 The Ales for Wiener Kind Structural Damped Systems

The ALEs of this kind of systems, suffers a bifurcation that depends on both the sign of the slope of the hysteresis cycle and the amplitude. Unfortunately, in a real system there is no information about the signal that goes into the hysteretic process. In the identification process, the unique information available is the system input  $x(t)$  and the hysteresis output  $q(t)$ .

This implies that the information about the slope of the hysteretic cycle is not available. This problem is overcome by use of the linear approximation  $y(t)$ . (equation 1). The slope is then obtained from the relationship  $y(i)$  vs  $q(t)$ .

Given the Polynomials  $Pu$  and  $Pv$  obtained from equations (3). The zero order signal is:

$$u_0(i) = Pu_4, \quad (4)$$

$$v_0(i) = Pv_4. \quad (5)$$

The first order signal is obtained from the same equations as:

$$u_1(i) = Pu_3y(i), \quad (6)$$

$$v_1(i) = Pv_3y(i). \quad (7)$$

On substitution in equation (1):

$$u_1(i) = C_1u_1(i-1) + C_2u_1(i-2) + C_3Pu_3x(i-1) + C_4Pu_3s(i-1), \quad (8)$$

$$v_1(i) = C_1v_1(i-1) + C_2v_1(i-2) + C_3Pv_3x(i-1) + C_4Pv_3s(i-1). \quad (9)$$

The number of operators is restrained by the maximum power of the polynomials (equations (3)). Therefore, only up to third order ALEs exists:

$$u_2(i) = \frac{Pu_2u_1^2(i)}{Pu_3^2}, \tag{10}$$

$$v_2(i) = \frac{Pv_2v_1^2(i)}{Pv_3^2}, \tag{11}$$

and third order are:

$$u_3(i) = \frac{Pu_1u_1^3(i)}{Pu_3^3}, \tag{12}$$

$$v_3(i) = \frac{Pv_1v_1^3(i)}{Pv_3^3}. \tag{13}$$

The use of one equation or the other depends on the sign of the slope of  $y(i)$ , i.e., the linear frequency system (Equation 1).

## 4 Structural Damping Model Simulation

### 4.1 Model Description

The simulated model is constructed as follows: The differential equation for a structural damping system from [14], is:

$$\ddot{y}(t) + i\omega_n\dot{y}(t) + \omega_n^2y(t) = Dx(t), \tag{14}$$

The solution for a forced fully integrable function is:

$$y(t) = \sum_{-\infty}^{\infty} \frac{D}{\omega_n^2 - \omega_i^2 + i\eta\omega_n\omega_i} e^{-i\omega_i t}, \tag{15}$$

$$y(t) = \sum_{-\infty}^{\infty} \frac{D}{\omega_n^2 - \omega_i^2 + i\eta\omega_n\omega_i} e^{-i\omega_i t}. \tag{16}$$

It is selected  $\eta=10$ ,  $\omega_n=500$ rd/sec,  $D=0.01$ . This signal goes into the hysteretic cycle which its saturation point is arbitrary selected at  $9.4867 \times 10^{-8}$ . The hysteretic cycle can be shown in figure (1).

### 4.2 Model Identification

The first step is to set a point in which the proportionality allows to have an mean square error (mse) [15] smaller than one, for the present case a level of an of  $mse=0.5044$  is found.

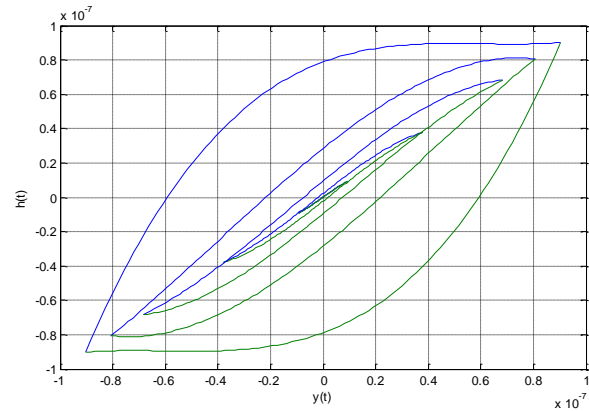


Fig. 1. Hysteretic cycle of the simulated system

A three input frequency signal is used  $\omega=350, 550$  and  $725$  rad/sec with amplitudes of  $0.02, 0.03$  and  $0.04$ m/s. By the use of the ARX algorithm described in [13] and the treatment for structural damping using an auxiliary variable as described in [12], the following model is obtained:

$$y(i) = 1.4149y(i - 1) - 0.9961y(i - 2) + 2.2325 \times 10^8x(i - 1) + -0.0083s(i - 1), \tag{17}$$

where  $s(i)$  is obtained from the direct and then the inverse of the Fourier transformation of equation (2).

The mse obtained is of  $0.2038\%$ . Which means an excellent agreement for this low level intensity. Figure 2 shows a graphical comparison.

The second step is now, to increment the intensity of the input signal using a sinusoidal function (frequency:  $225$ rad/sec) with an amplitude of  $1.25$  m/s. the proportionality exhibits an mse of  $1.3\%$ .

Let's calculate  $y(i)$  from equation (17). Then, when plotted with the actual system output  $q(i)$  the hysteretic cycle is observed Figure 3.

The signal is divided in two parts, each one related with the sign of the Figure 3 graphics slope. Each part is approximated by a three degree polynomial as in equations (2, 3). Unfortunately,  $y(t)$  or its equivalent discrete  $y(i)$  is not available.

It is the necessary to take advantage of the proportionality property of the linear systems. It makes necessary to be able to control the input and set at low level as for example:

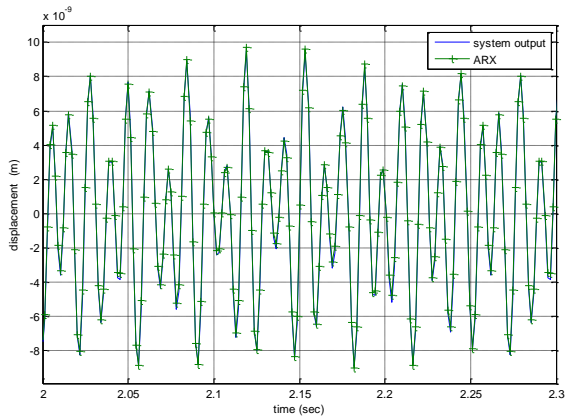


**Fig. 2.** Linear approximation for low level excitation of the modeled system

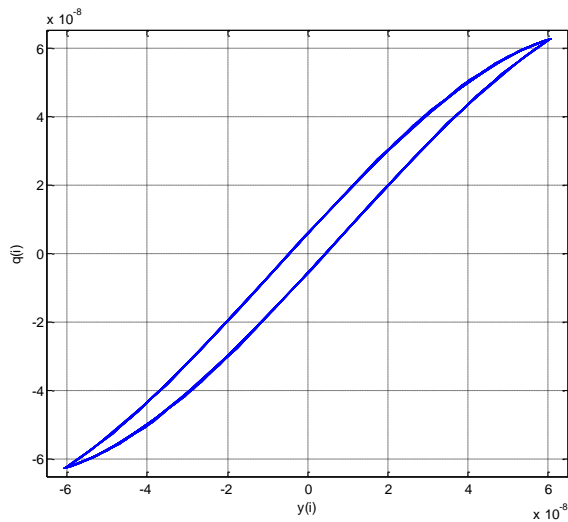


**Fig. 3.** Graphics of  $y(i)$  vs  $q(i)$ . The graphics shows the hysteresis. Initial points are removed

$$xr(i) = \frac{x(i)}{r},$$

where  $r > 1$  so that  $xr$  is well into the linear response of the linear in frequency sub-system. Let's the response to be  $yr(i)$ , then:

$$y(i) = r yr(i).$$

The coefficients of the polynomials are then:

$$Pu = [-7.0862 \times 10^{13}, -1.2595 \times 10^6, 1.2789, 5.4979 \times 10^{-9}]$$

$$Pv = [-7.1621 \times 10^{13}, 1.2036 \times 10^6, 1.2800, -5.4211 \times 10^9]$$

With this information, there is a zero order operators from equations (4) and (5):

$$u_0(i) = 5.4979 \times 10^{-9},$$

$$v_0(i) = -5.4211 \times 10^{-9},$$

the first order Associated Linear Equations (ALEs) are from equations (3):

$$u_1(i) = 1.4149u_1(i-1) - 0.9961u_1(i-2) + 2.85951 \times 10^{-8}x(i-1) - 0.0083s(i-1), \quad (18)$$

$$v_1(i) = 1.4149v_1(i-1) - 0.9961v_1(i-2) + 2.8551 \times 10^{-8}x(i-1) - 0.0083s(i-1). \quad (19)$$

The higher order inverse operators are:

$$u_2(i) = -1.2595 \times 10^6 \frac{u_1^2}{1.2789^2}, \quad (20)$$

$$v_2(i) = 1.2036 \times 10^6 \frac{v_1^2}{1.2800^2}, \quad (21)$$

$$u_3(i) = -7.0862 \times 10^{13} \left[ \frac{u_1^3}{1.2789^3} \right], \quad (22)$$

$$v_3(i) = -7.1621 \times 10^{13} \frac{v_1^3}{1.2800^3}. \quad (23)$$

The use of  $u_i(i)$  or  $v_i(i)$  depends on the sign of the slope of  $h(i)$ . For up to the first order Volterra operator, the mse is of 9.8494% the full three order sum of Volterra operators gives an mse=1.2988%.

## 5 The Inverse Volterra Operators for Structural Damped and Wiener

From now on, when talking about an operator it can be referred by a low case letter, e.g. either  $u(i)$  or  $v(i)$  or by a bold capital letter, e.g. **H**.

The capital letter is referred to the operator process and it is always the same, independently of its input.

Lower case is referred to a particular signal that is the output of the operator process and it varies according with the input.

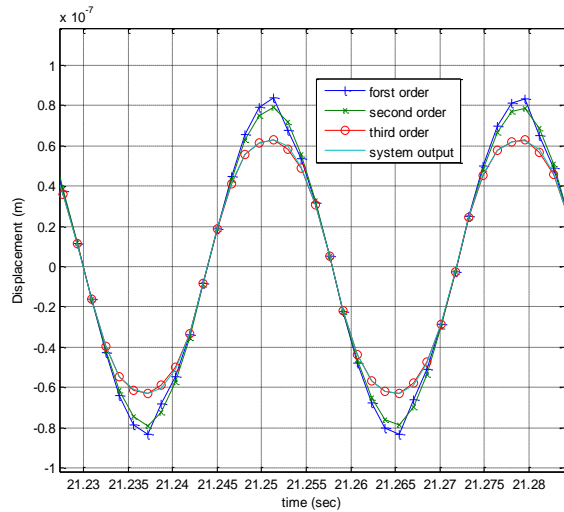


Fig. 4. Comparison between the hysteretic output against the Volterra prediction

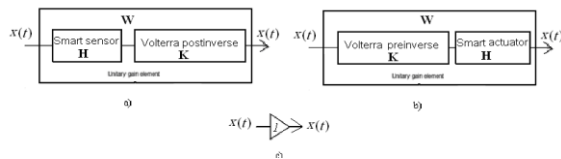


Fig. 5. Open loop control by the inverse Volterra: (a) predistortion for sensors, (b) equalization for actuators

The equalization strategy is proposed for sensors in [11] as an open loop control. Application on Wiener system can be found in [10]. Figure (5) shows how the equalization is implemented.

In [11], because it is not always possible to eliminate the DC term, it is recommended to let the DC to cross all the way out through the inverse system.

In the hysteresis cycle, the DC is switching and therefore is not properly a constant term in the system, it is rather a square signal that is adding to the linear response, and therefore the term of order zero is rather a part of the first order response. The system output from (2, 3) is either:

$$u(i) = u_0(i) + u_1(i) + u_2(i) + u_3(i),$$

or,

$$v(i) = v_0(i) + v_1(i) + v_2(i) + v_3(i).$$

The DC can be directly subtracted before enter the preinverse.

For low excitation level, the inverse Volterra consists in just one operator  $z_1(t)$  as explain in [8] The discrete ALE, is the inverse operator of the direct first order operator expressed by equation (1), as explained in the same reference, the first order inverse ALE is then:

$$z_1(i-1) = \frac{1}{C_3} y(i) - \frac{C_1}{C_3} y(i-1) - \frac{C_2}{C_3} y(i-2) - \frac{C_4}{C_3} s(i-1). \tag{24}$$

Equivalently, for higher input level, the first order inverse is:

$$z_{u1}(i-1) = \frac{1}{C_3 P u_3} q(i) - \frac{C_1}{C_3 P u_3} q(i-1) - \frac{C_2}{C_3 P u_3} q(i-2) - \frac{C_4}{C_3 P u_3} s_q(i-1), \tag{25}$$

$$z_{v1}(i-1) = \frac{1}{C_3 P v_3} q(i) - \frac{C_1}{C_3 P v_3} q(i-1) - \frac{C_2}{C_3 P v_3} q(i-2) - \frac{C_4}{C_3 P v_3} s_q(i-1), \tag{26}$$

where the auxiliary variable is obtained from  $q(i)$  defined as:

$$s_q(t) = i \text{ sign}(\omega) q(t),$$

$q(i)$  slope sign determines if equation (25 or 26) is used.

The second order is obtained as in [17]. From Figure 5 the inverse Volterra operator is:

$$z_2(t) = -K_1[H_2\{K_1[q(t)], K_1[q(t)]\}], \tag{27}$$

where  $H_i$  (equations (89)) and  $K_i$  (equations (25, 26)) are the direct and inverse operators. Then the output are the operators  $z_{u1}$  an  $z_{v1}$ ,  $H_2$  is governed by equations (11, 12). According with equation (27), the input into  $H_2$  is:

$$u_1(i) = \mathbf{H}_{1u}[\mathbf{K}_{u1}[q(i)]], \quad (28)$$

$$v_1(i) = \mathbf{H}_{v1}[\mathbf{K}_{v1}[q(i)]], \quad (29)$$

as  $\mathbf{H}_1$  and  $\mathbf{K}_1$  are inverse systems:

$$u_1(i) = q(i), \quad (30)$$

$$v_1(i) = q(i), \quad (31)$$

on substitution into equations (11, 12):

$$u_2(i) = \frac{Pu_2}{Pu_3^2} q(i)^2, \quad (32)$$

$$v_2(i) = \frac{Pv_2}{Pv_3^2} q(i)^2. \quad (31)$$

At its time equations (30, 31) are the input into the first order system  $\mathbf{K}_1$  as equation (27) indicates, then from equations (25, 26):

$$z_{u1}(i-1) = \frac{1}{C_3Pu_3} u_2(i) - \frac{C_1}{C_3Pu_3} u_2(i-1) - \frac{C_2}{C_3Pu_3} u_2(i-2) - \frac{C_4}{C_3} s_u(i-1), \quad (32)$$

$$z_{v1}(i-1) = \frac{1}{C_3Pv_3} v_2(i) - \frac{C_1}{C_3Pv_3} v_2(i-1) - \frac{C_2}{C_3Pv_3} v_2(i-2) - \frac{C_4}{C_3} s_v(i-1), \quad (33)$$

where:

$$s_u(i) = i \operatorname{sign}(\omega) u_2(i),$$

and:

$$s_v(t) = i \operatorname{sign}(\omega) v_2(t).$$

Following equation (27) the second order inverse operator is simply:

$$z_{u2}(i-1) = -z_{u1}(i-1), \quad (34)$$

$$z_{v2}(i-1) = -z_{v1}(i-1). \quad (35)$$

For the third order operator, as it is treated in [17]:

$$z_3(t) = -\mathbf{K}_1[\mathbf{H}_3\{\mathbf{K}_1[q(t)], \mathbf{K}_1[q(t)], \mathbf{K}_1[q(t)]\}] - 2\mathbf{K}_1[\mathbf{H}_2\{\mathbf{K}_1[q(t)], \mathbf{K}_2[q(t)], q(t)\}]. \quad (36)$$

The first term of equation (36) undertakes a similar treatment as for the second order operator, and third order are:

$$u_3(i) = \frac{Pu_1}{Pu_3^3} q(i)^3, \quad (37)$$

$$v_3(i) = \frac{Pv_1}{Pv_3^3} q(i)^3, \quad (38)$$

then signal goes into the first order operator:

$$z_{u1}(i-1) = \frac{1}{C_3Pu_3} u_3(i) - \frac{C_1}{C_3Pu_3} u_3(i-1) - \frac{C_2}{C_3Pu_3} u_3(i-2) - \frac{C_4}{C_3} s_u(i-1), \quad (39)$$

$$z_{v1}(i-1) = \frac{1}{C_3Pv_3} v_3(i) - \frac{C_1}{C_3Pv_3} v_3(i-1) - \frac{C_2}{C_3Pv_3} v_3(i-2) - \frac{C_4}{C_3} s_v(i-1), \quad (40)$$

where,

$$s_u(i) = i \operatorname{sign}(\omega) u_3(i),$$

and

$$s_v(i) = i \operatorname{sign}(\omega) v_3(i),$$

$$z_{u3}(i-1) = -z_{u1}(i-1) + \text{second term}, \quad (41)$$

$$z_{v3}(i-1) = -z_{v1}(i-1) + \text{second term}. \quad (42)$$

Now, for the second term of equation (36) one has:

$$2\mathbf{K}_1[\mathbf{H}_2\{\mathbf{K}_1[q(t)], \mathbf{K}_2[q(t)], q(0t)\}]. \quad (43)$$

The second argument of  $\mathbf{H}_2$  is:

$$\mathbf{K}_2[q(t), q(t)] = -\mathbf{K}_1[\mathbf{H}_2\{\mathbf{K}_1[q(t)], \mathbf{K}_1[q(t)]\}] = z_2(t). \quad (44)$$

Then, (40) is now:

$$2\mathbf{K}_1[\mathbf{H}_2\{z_1(t), z_2(t)\}]. \quad (45)$$

Equation (28, 29) should be rewritten as follows:

$$u_2(i) = \frac{Pu_2u_1(i)u_1(i)}{Pu_3^2}, \quad (46)$$

$$v_2(i) = \frac{Pv_2v_1(i)v_1(i)}{Pv_3^2}. \quad (47)$$

Thought the abuse of the nomenclature, in equations (11, 12)  $u(i)$  and  $v(i)$  are two different signals as the input in each equation as the input into the operator  $\mathbf{H}_1$  is different for each factor, i.e.:

$$u_2(i) = \frac{Pu_2\mathbf{H}_{1u}[z_1(t)]\mathbf{H}_{1u}[z_2(t)]}{Pu_3^2}, \quad (48)$$

$$v_2(i) = \frac{Pv_2\mathbf{H}_{1v}[z_1(t)]\mathbf{H}_{1v}[z_2(t)]}{Pv_3^2}. \quad (49)$$

The first factor is simply the sensor system output:

$$u_2(i) = \frac{Pu_2q(i)\mathbf{H}_{1u}[z_2(i)]}{Pu_3^2}, \quad (50)$$

$$v_2(i) = \frac{Pv_2q(i)\mathbf{H}_{1v}[z_2(i)]}{Pv_3^2}. \quad (51)$$

The second factor can be obtained by the handling equation (43) as follows, eliminating inverse operators:

$$\begin{aligned} \mathbf{H}_{1v}[z_2(i)] \\ = -\mathbf{H}_{1v}[\mathbf{K}_{v1}[\mathbf{H}_{v2}\{\mathbf{K}_{v1}[q(t)], \mathbf{K}_{v1}[q(t)]\}]] \end{aligned} \quad (52)$$

$$\mathbf{H}_{1v}[z_2(i)] = -[\mathbf{H}_{v2}\{\mathbf{K}_{v1}[q(t)], \mathbf{K}_{v1}[q(t)]\}].$$

The second order Volterra ALE is from equations (11, 12):

$$\mathbf{H}_{1u}[z_2(i)] = -\frac{Pu_2}{Pu_3^2}q(i)^2, \quad (53)$$

$$\mathbf{H}_{1v}[z_2(i)] = -\frac{Pv_2}{Pv_3^2}q(i)^2. \quad (54)$$

Equations (50, 51) are then:

$$u_2(i) = -\frac{Pu_2^2q(i)^3}{Pu_3^4}, \quad (55)$$

$$v_2(i) = -\frac{Pv_2^2q(i)^3}{Pv_3^4}. \quad (56)$$

The second term  $2\mathbf{K}_1[\mathbf{H}_2\{z_1(t), z_2(t)\}]$  of equation (43) is then:

$$\begin{aligned} z_{0u1}(i-1) = & \frac{1}{C_3Pu_3}u_2(i) - \frac{C_1}{C_3Pu_3}u_2(i-1) \\ & - \frac{C_2}{C_3Pu_3}u_2(i-2) \\ & - \frac{C_4}{C_3}s_u(i-1), \end{aligned} \quad (57)$$

$$\begin{aligned} z_{0v1}(i-1) = & \frac{1}{C_3Pv_3}v_2(i) - \frac{C_1}{C_3Pv_3}v_2(i-1) \\ & - \frac{C_2}{C_3Pv_3}v_2(i-2) \\ & - \frac{C_4}{C_3}s_v(i-1). \end{aligned} \quad (58)$$

On substitution in equation (43), the third order operator results to be:

$$z_{u3}(i-1) = -z_{u1}(i-1) - 2z_{0u1}(i-1), \quad (57)$$

$$z_{v3}(i-1) = -z_{v1}(i-1) - 2z_{0v1}(i-1). \quad (58)$$

As a difference from the direct Volterra operators, the lower order inverse Volterra operators generates signals of higher harmonic order and therefore it is necessary the addition of higher order inverse operators.

Then, the inverse Volterra is an infinite series. The present work is delimited to the third order.

## 6 Inverse Volterra on the Simulated Sensor System

### 6.1 Low Level Excitation

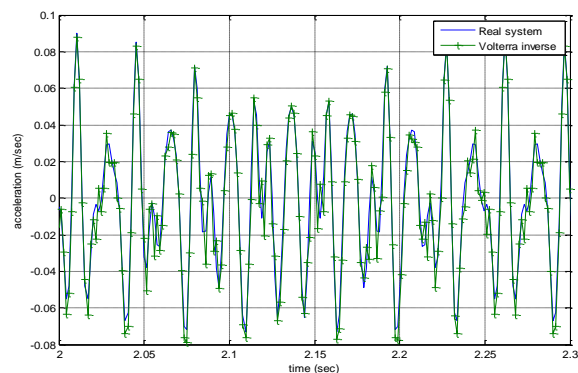
For low level excitation, the inverse Volterra can be composed of only the first order operator and it converges to the inverse obtained directly from equation (24).

Figure 6 shows the first order inverse operator against the low level input signal, the mse is only of 0.8%.

### 6.2 Higher Level Excitation

Equation (37) from the data in the section in which the identification is carried out:

$$\begin{aligned} z_{u1}(i-1) \\ = \frac{v_1(i) - 1.3643v_1(i-1) + .9268v_1(i-2) - .054u(i-1)}{2.85951 \times 10^8} \end{aligned}$$



**Fig. 6.** Equalization strategy, the input acceleration, the acceleration measured

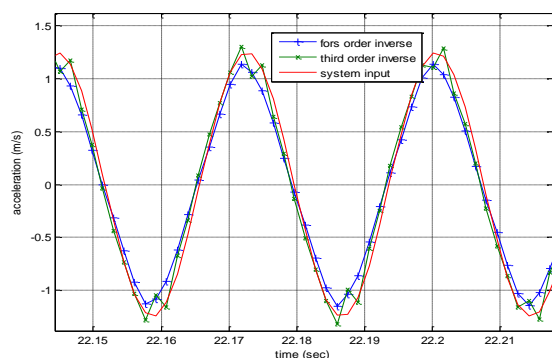


**Fig. 7.** Equatization strategy, for nonlinear response. The inverse Volterra compared with the original input signal

$$z_{v1}(i-1) = \frac{v_1(i) - 1.4149v_1(i-1) + 0.9961v_1(i-2) - 0.0083u(i-1)}{2.8551 \times 10^8}$$

The second is obtained from equation (27), Equation (30) is then:

$$u_2(i) = \frac{-1.2595 \times 10^6}{1.2789^2} q(i)^2,$$

$$v_2(i) = \frac{1.2036 \times 10^6}{1.2800^2} q(i)^2.$$

On substitution in equation (32, 33), the second order inverse is given by (34, 35). Equation (56, 57) gives the third order inverse. The same input signal that is used for identifying the hysteresis cycle, section 4.2, is used here, Figure 7 shows the inverse Volterra performance

for this input level. The first order inverse gives an mse of 2.8377 and the full inverse Volterra gives an mse of 1.736.

## 7 Conclusions

It has been applied an equalization open loop control using the inverse Volterra operator on a simulated sensor system. The simulation response is obtained out from a structural damping model (linear in frequency) using its exact solution and adding a hysteretic element that is the response of the sensing element that measures the structure deformation. This is a very close behavior of an accelerometer with a piezoelectric element.

To implement the inverse Volterra, a model of the simulated system has to be constructed. This is done by assign a Wiener model to the system. Because of the hysteresis, the system becomes amplitude dependence, therefore the system is not a real Volterra system kind, However because of the nonlinearity is out of the structure system, the Wiener model can be modified to have variable nonlinear coefficients.

The hysteresis is identified as two cubic functions, each one modeling the positive and negative slope of the hysteresis.

The model to assign presents another problem because the system is not properly linear but linear in frequency, so the model of the simulated system has to be modified by an auxiliary variable that accounts for the complex rigidity.

For low level, the system is identified as a linear in frequency just as it has been identified in [10], the identification is satisfactory, and the Volterra inverse of first order is enough accurate to recover the sensor input.

For high input level, the Wiener model produces three Associated Linear Equations, each one for each harmonic component in the measured signal (output signal), and a ALE of zero order. The model result to suffice to produce a very good agreement with the output system. As a difference from [12] in which the system model is not to be used for prediction purposes (as it is function of the auxiliary variable that comes from the output) and therefore only used constructing the Volterra inverse, in the present work can be

used for response prediction as the auxiliary variable is obtained from proportionality of the response at low level.

The inverse Volterra is trunked to third order and for the hysteresis level used in here, the sensor input is recovered with high accuracy. The open loop control presented here demonstrates to be adequate for system with hysteresis.

## References

1. **Uchino, K. (1998).** Piezoelectric ultrasonic motors: Overview. *Smart Materials and Structures*, Vol. 7, No. 3, pp. 273–285. DOI: 10.1088/0964-1726/7/3/002.
2. **Aguirre, G., Janssens, T., Van Brussel, H., Al-Bender, F. (2012).** Asymmetric-hysteresis compensation in piezoelectric actuators. *Mechanical Systems and Signal Processing*, Vol. 30, pp. 218–231. DOI: 10.1016/j.ymssp.2011.11.012.
3. **Li, Y., Tong, S., Li, T. (2012).** Adaptive fuzzy output feedback control of MIMO nonlinear uncertain systems with time-varying delays and unknown backlash-like hysteresis. *Neurocomputing*, Vol. 93, pp. 56–66. DOI: 10.1016/j.neucom.2012.04.004.
4. **Farah, N., Talib, M.H.N., Ibrahim, Z., Mat Isa, S.N., Lazi, J.M. (2017).** Variable hysteresis current controller with fuzzy logic controller based induction motor drives. 7th IEEE International Conference on System Engineering and Technology, pp. 122–127. DOI: 10.1109/ICSEngT.2017.8123432.
5. **Talib, M.H.N., Mat Isa, S.N., Hamidon, H.E., Ibrahim, Z., Rasin, Z. (2016).** Hysteresis current control of induction motor drives using dSPACE DSP controller. *IEEE International Conference on Power and Energy*, pp. 552–527. DOI: 10.1109/PECON.2016.7951617.
6. **Trong-Tai, N., Kwan-Ahn, K. (2012).** A hysteresis functional link artificial neural network for identification and model predictive control of SMA actuator. *Journal of Process Control*, Vol. 22, No. 4, pp. 766–777. DOI: 10.1016/j.jprocont.2012.02.007.
7. **Magneval, M., Josefsson, A., Ahlin, K. (2007).** Parameter Estimation of Hysteresis Elements Using Harmonic Input.
8. **Ceravolo, R., Demarie, G.V., Erlicher, S. (2009).** Instantaneous identification of Bouc-Wen-type hysteretic systems from seismic response data. *Key Engineering Materials*, Vol. 347, pp. 331–338. DOI: 10.4028/www.scientific.net/KEM.347.331.
9. **Vazquez-Feijoo, J.A., Worden, K., Stanway, R., Juárez-Rodríguez, N. (2007).** Transformation of a sensor or actuator system into a unitary gain element. *Mechanical Systems and Signal Processing*, Vol. 2, No. 18, pp. 3088–3107. DOI: 10.1016/j.ymssp.2007.03.008.
10. **García-Aparicio, E.A., Cortés-Lerín, V., Vazquez-Feijoo, J.A., Matadamas-Ortiz, P.T. (2013).** Associated linear equations for the wiener kind of Volterra systems. 15th Asia Pacific Vibration Conference, pp. 66–72.
11. **Vazquez-Feijoo, J.A., Worden, K., Stanway, R. (2006).** Analysis of time-invariant systems in the time and frequency domain by associated linear equations. *Mechanical Systems and Signal Processing*, Vol. 20, No. 4, pp. 896–919. DOI: 10.1016/j.ymssp.2005.03.004.
12. **Vazquez-Feijoo, J.A., Matadamas-Ortiz, P.T., Rios-Olivera, V.J. (2013).** Structural damping system controlled by the Volterra inverse and a modal transformation. *ICCECT International Conference on Control Engineering and Communication Technology*, pp. 224–227. DOI: 10.1109/ICCECT.2012.104.
13. **Billings, S.A., Chen, S., Korenberg, M.J. (1989).** Identification of MIMO non-linear systems using a forward-regression orthogonal estimator. *International Journal of Control*, Vol. 49, No. 6, pp. 2157–2189. DOI: 10.1080/00207178908559767.
14. **Liang, Z., Lee, G.C., Dargush, G.F., Song, J. (2011).** Structural damping: Applications in seismic response modification (advances in earthquake engineering). CRC Press Taylor & Francis Group.
15. **Worden, K., Tomlinson, G.R. (2000).** Nonlinearity in structural dynamics: Detection, identification and modelling. Taylor & Francis.
16. **Vazquez-Feijoo, J.A., Worden, K., Rodríguez, N.J., Pozos-Osorio, J., Matadamas-Ortiz, P. (2009).** Analysis and control of nonlinear systems with DC terms. *Nonlinear Dynamics*, Vol. 58, No. 4, pp 753–775. DOI: 10.1007/s11071-009-9516-x.
17. **Schetzen, M. (1980).** The Volterra and Wiener theories of nonlinear systems. Wiley-Interscience Publications.

*Article received on 29/07/2020; accepted on 25/03/2021.  
Corresponding author is Vladimir Cortés Lerín.*